Activating Water and Hydrogen by Ligand-Modified Uranium and Neptunium Complexes: A DFT Study

Olajumoke Adeyiga[#], Dipak Panthi[#], Olabisi Suleiman[#], Dillon Stetler, Ryan W. Long and Samuel O. Odoh*

Department of Chemistry, University of Nevada Reno, 1664 N. Virginia Street, Reno, NV 89557-0216

Email Addresses:

oadeyiga@unr.edu

dpanthi@unr.edu

osuleiman@unr.edu

dstetler@nevada.unr.edu

ryanlong@nevada.unr.edu

sodoh@unr.edu

ABSTRACT: Organometallic uranium complexes that can activate small molecules are well known. In contrast, there are no known organometallic trans-uranium species capable of small-molecule transformations. Using density functional theory, we previously showed that changing actinide-ligand bonds from U-O groups to Np-N- (amide/imido) bonds makes redox small-molecule activation more energetically favorable for Np species. Here, we determine how *general* this ligand-modulation strategy is for affecting small-molecule activation in Np species. We focus on two reactions, one involving redox transformation of the actinide(s) and the other involving no change in the oxidation state of the actinide(s). Specifically, we considered the hydrogen evolution reaction (HER) from H_2O by actinide tris-aryloxide species. We also considered H_2 capture and hydride transfer by actinide siloxide and silylamide complexes. For the HER, the barriers for Np(III) systems are much higher than those of U(III). The overall reaction energies are also much worse. An-O → An-N substitutions marginally improve the barriers by 1-4 kcal/mol and more substantially improve the reaction energies by 9-15 kcal/mol. For H_2 capture and hydride transfer, the reaction energies for the U and Np species are similar. For both actinides, *like-for-like* An-O → An-N substitutions lead to improved reaction energies. Interestingly, in a recent report, it seemingly appears that U-O (siloxide) → U-N (silylamide) leads to complete shutdown of reactivity for H_2 capture and hydride transfer. This observation

is reproduced and explained with calculations. The ligand environments of the siloxide and silylamide that were compared are vastly different. The steric environment of the siloxide is conducive for reactivity while the particular silylamide is not. We conclude that small-molecule activation with organometallic neptunium species is achievable with a guided choice of ligands. Additional emphasis should be placed on ligands that can allow for improved transition state barriers.

1. INTRODUCTION

Approaches to activate small molecules like N_2, H_2O, CH_4 and CO_2 in order to generate energy and industrially-important chemical feedstocks are at the cutting edge of research in inorganic, organometallic and materials chemistry. These molecules are often activated with transition metal complexes and surfaces. Recent investigations have however shown that uranium (U) can also effect small-molecule transformations. U complexes can activate H_2, CH_4, H_2O, CO, NO and N_2.[1-20] Although many of these transformations are stoichiometric reactions, they remain important nonetheless. A detailed understanding of the thermodynamics, mechanisms, and kinetics of these transformations can provide insights towards the design of catalytic platforms. Additionally, catalytic transformations of small-molecules with U species have the potential to alter the use, separation, storage and public perception of nuclear waste materials. Nuclear waste forms also contain trans-uranium elements like neptunium (Np), plutonium (Pu) and americium (Am). However, there are no reports on the ability of trans-uranium complexes to effect small-molecule redox transformations.[21,22] Thus, there is interest in the development of trans-uranium complexes that can activate small molecules in a similar manner to their U analogues.

Recently, it was shown using density functional theory (DFT) calculations that, while a U complex could perform a four-electron reduction of N_2, $N_2 \rightarrow N_2^{4-}$, analogous Np and Pu species could not. The Np and Pu analogues could not effect this transformation due to a shift in the balance of redox potentials.[17] The U complex was initially synthesized and characterized by Falcone et al. They also characterized its ability to activate N_2 to N_2^{4-}.[9] We showed that modulation of the actinide-ligand bonds as well as the ligand framework can be used to make $N_2 \rightarrow N_2^{4-}$ favorable for the Np analogue. Specifically, changing the Np-O bonds to metal-imido Np-NH groups favored $N_2 \rightarrow N_2^{4}$.[17] Herein, we examine whether Np-O → Np-N substitution is useful in the activation of *other* small molecules.

In this work, we use DFT computations to study the electrocatalytic evolution of hydrogen (H_2) from water by actinide complexes, Scheme 1. We considered systems that are based on the previously reported U(III) trisaryloxide complex, [((^{Ad,Me}ArO)$_3$*mes*)U] where *mes* = mesityl, *Ad* = adamantyl and *Me* = methyl. [((^{Ad,Me}ArO)$_3$*mes*)U] evolves H_2 from water with a turnover frequency comparable to state-of-the-art transition-metal systems.[12,13] The mechanism for H_2 evolution from water by this U complex involves two hydrogen atom abstraction steps as well as rare terminal pentavalent U=O and U-OH complexes, Scheme 1.[23-27] This reaction mechanism is quite similar to the one previously reported by Meyer et al.[12,13] The pentavalent U=O complex comproportionates with [((^{Ad,Me}ArO)$_3$*mes*)U].OH_2 to yield a tetravalent U-OH species which is then electrocatalytically reduced in the experiments setup. We compare the stoichiometric process for H_2 evolution via the intramolecular insertion mechanism, Scheme 1, by [((^{Ad,Me}ArO)$_3$*mes*)U], [((^{Ad,Me}ArNH)$_3$*mes*)U], [((^{Ad,Me}ArO)$_3$*mes*)Np] and [((^{Ad,Me}ArNH)$_3$ *mes*)Np] species.

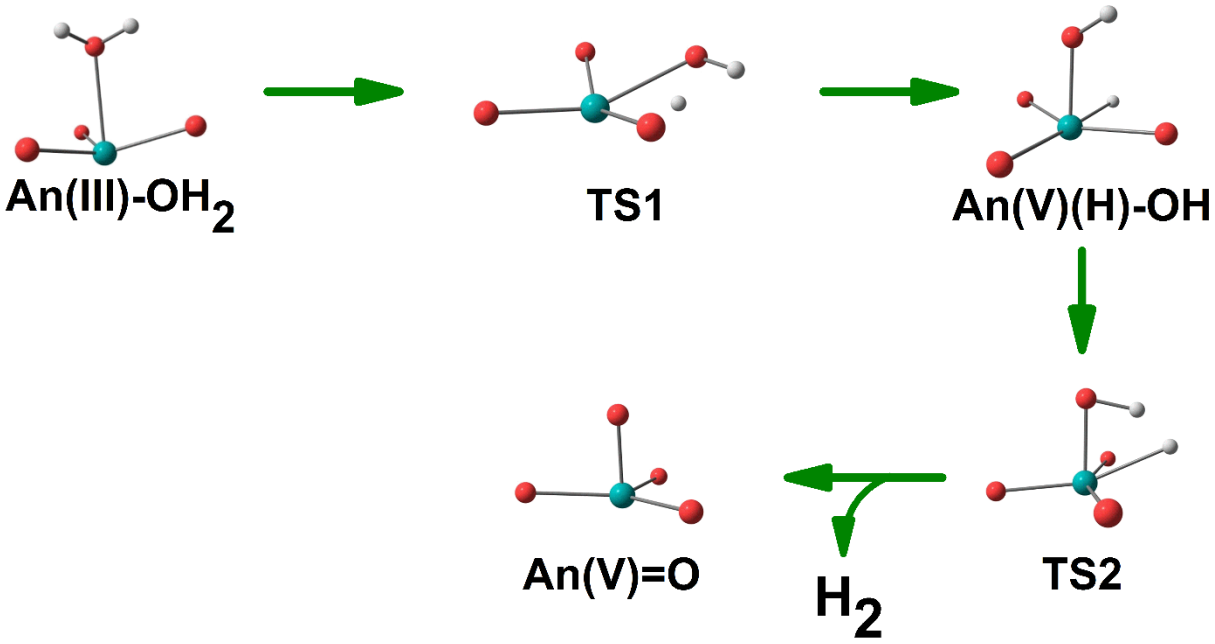

Scheme 1: Mechanism for hydrogen evolution from water by An^{3+} trisaryloxide species. The ligands are not shown to allow for clarity.

Additionally, a recent experimental report has revealed interesting insights into small-molecule activation by uranium amide (U-NR_2) complexes. Specifically, reactivity with small molecules (CO, CO_2 and H_2) was demonstrated by the siloxide complex while the silylamide species showed no reactivity.[16] These results would suggest that An-O → An-N ligand substitution may

not always lead to improved reactivities. However, close examination indicates that the ligand environments of these species are quite different. Specifically, there is a U-O-Si spacer between U and the O-*t*-Bu groups in the siloxide whereas the $N(SiMe_3)_2$ ligands are rather close-in on the U center in the case of silylamide, Figure 1. It is thus important that we ascertain that our computational protocol can adequately distinguish between cases in which significant ligand modification leads to improved or diminished reactivities. We also seek to determine whether a *like-for-like* O → NH substitution in U-OSi(O-*t*-Bu)$_3$ framework (to U-N(H)Si(O-*t*-Bu)$_3$) would restore reactivity with H_2. These questions are also explored for the analogous Np species. To this end, we have considered H_2 capture and hydride transfer by bis-uranium nitride (U-N-U) siloxide or silylamide complexes that were characterized by Palumbo et al., Figure 1.[16] The two U centers in these complexes are in the +4 oxidation state, bridged by a nitride and are coordinated to three siloxide/silylamide groups, with the total charge balanced by a tetrabutyl-ammonium cation, NBu_4^+. We studied the anionic forms of these complexes, without

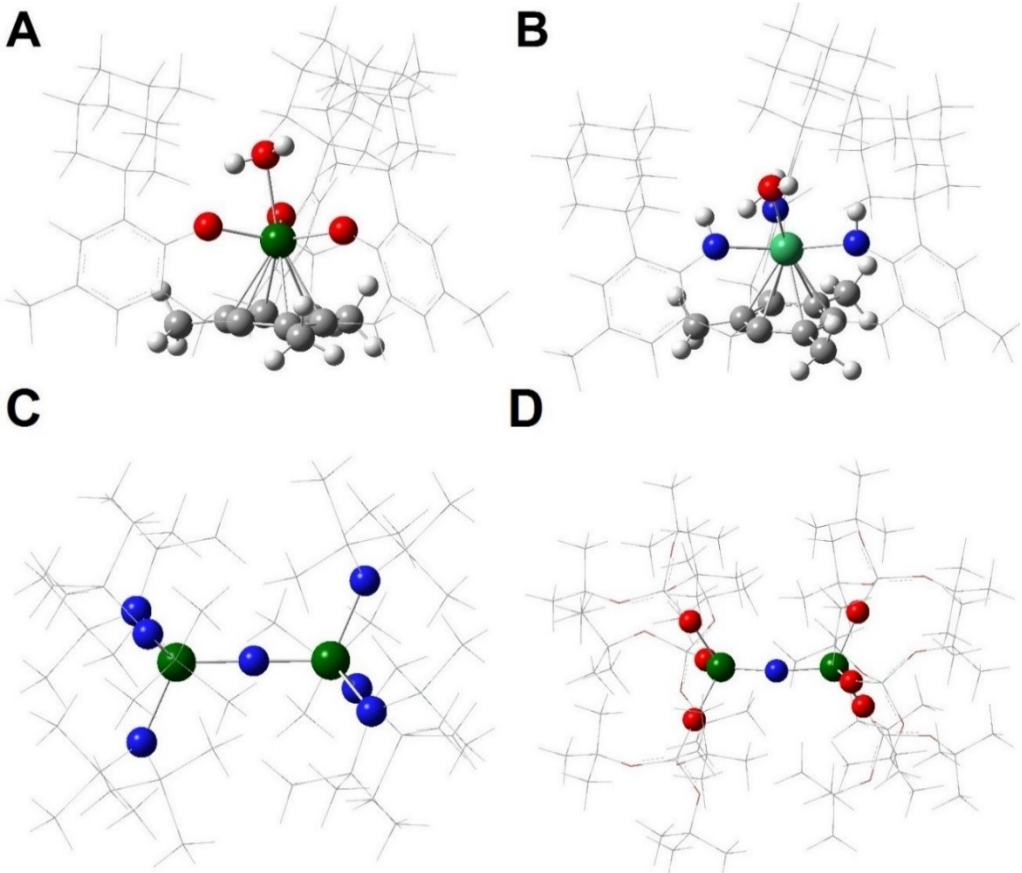

Figure 1: Structures of **A.** [((^{Ad,Me}ArO)$_3$*mes*)U].OH_2 **B.** [((^{Ad,Me}ArNH)$_3$*mes*)Np].OH_2 **C.** [(N)U-N-U(N)]$^-$ and **D.** [(O)U-N-U(O)]$^-$. The ligands are depicted with wireframes for better visibility. **A** and **B** are studied for HER while **C** and **D** are studied for H_2 capture and hydride transfer.

NBu_4^+. These are labelled as $[(O)U\text{-}N\text{-}U(O)]^-$ (for the siloxide, $OSi(O\text{-}t\text{-}Bu)_3$) and $[(N)U\text{-}N\text{-}U(N)]^-$ (for the silylamide, $N(SiMe_3)_2$), for simplicity, Figure 1. We emphasize again that the ligand frameworks of the siloxide and silylamide are quite different, Figure 1.

2. COMPUTATIONAL DETAILS

We optimized the structures of the tris-aryloxide and bis-actinide nitride complexes, Figure 1, in the gas phase with all-electron L1 (double-ζ) extended basis sets at the scalar relativistic level with the Priroda code. These calculations were performed with the PBE functional. The description of the basis sets and scalar-relativistic approach have been previously described.[28-30] Single-point calculations accounting for spin-orbit coupling and/or solvent effects were subsequently performed with the ADF code.[31,32] We used Slater-type triple-ζ basis sets with two polarization functions, TZ2P, and the PBE generalized gradient approximation exchange-correlation DFT functional.[33,34] This functional provides accurate results for predicting the redox reactivity and ionization potentials of actinide species.[35-41] Dispersion effects were included in these calculations with the DFT-D3 scheme[42,43] supplemented with the Becke-Johnson damping scheme, DFT-D3(BJ).[44] Scalar-relativistic effects were accounted for with the zeroth order regular approximation (ZORA) approach.[45] The TZ2P basis sets used were adapted for use with ZORA.[46,47] The actinide tris-aryloxides were studied for the HER experiments which were performed in solution (THF). In contrast, the bis-actinide-nitride species were studied for H_2 capture and were studied in the gas phase, in accordance with the experiments of Palumbo et al.[16] The spin-orbit DFT calculations were performed in the non-collinear unrestricted fashion at the PBE-D3(BJ)/TZ2P level while still employing the ZORA approach. Calculations in the solvent phase, specifically in THF were carried out with the SM12 implicit solvation model.[48,49] This is reasonable as the electrocatalytic experiments of Halter et al. were performed in THF.[12,13] The dielectric constant of THF was taken as 7.58 while the radius of the solvent molecules was taken as 3.18 Å. Unless otherwise stated, our discussions are based on calculations at the PBE-D3BJ/TZ2P level.

3. RESULTS AND DISCUSSION

3.1. Hydrogen Evolution from Water: The mechanism for H_2 evolution from the aquo ligand in $[((^{Ad,Me}ArO)_3mes)U].OH_2$, $[((^{Ad,Me}ArO)_3mes)Np].OH_2$ and $[((^{Ad,Me}ArNH)_3mes)Np].OH_2$ are compared in Figure 2. The mechanistic steps are similar to those reported by Meyer et al.[12,13]

Interestingly, our calculation shows that the first hydrogen-atom abstraction step is the rate-determining step (RDS) for [((^{Ad,Me}ArO)$_3$*mes*)U].OH$_2$. This is in contrast to Meyer et al. who predicted the second transition state, TS2, as the rate-limiting barrier. They found that TS2 is 24.6 kcal/mol above the starting complex, [((^{Ad,Me}ArO)$_3$*mes*)U].OH$_2$. This is rather high for a

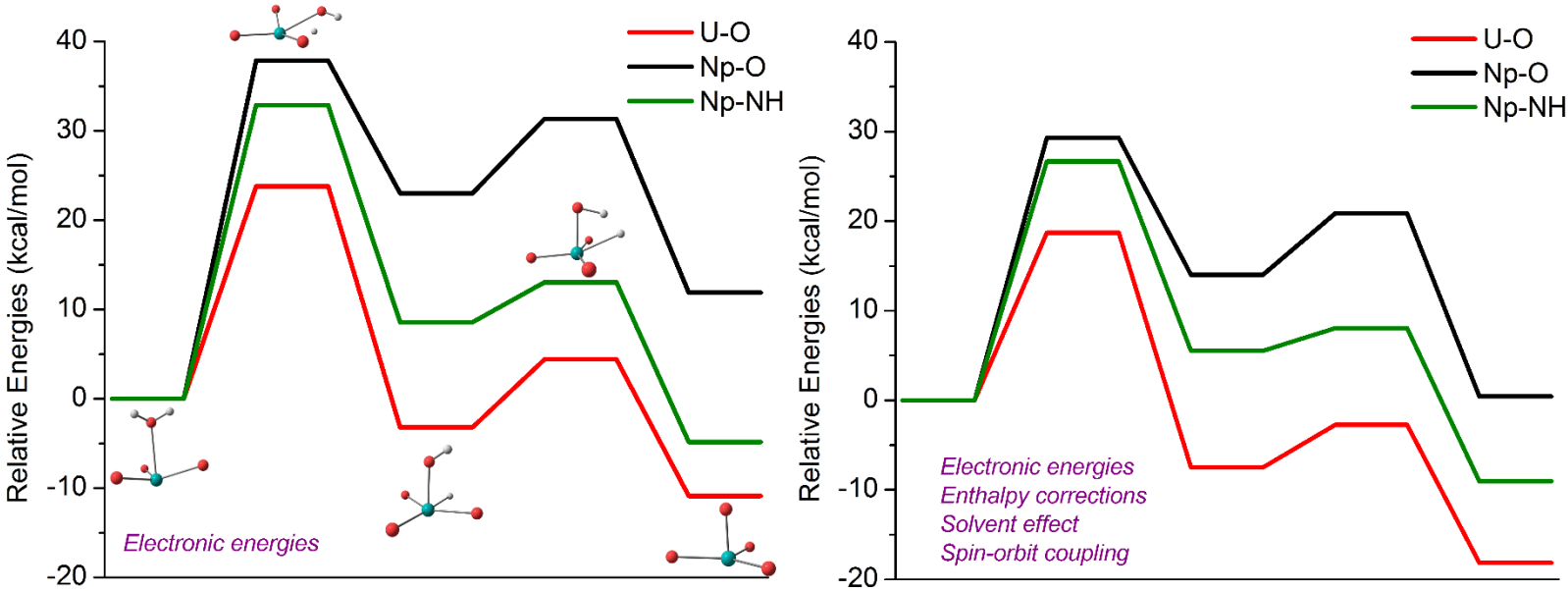

Figure 2: Overall reaction energy profiles for [((^{Ad,Me}ArO)$_3$*mes*)U].OH$_2$, [((^{Ad,Me}ArO)$_3$*mes*)Np].OH$_2$ and [((^{Ad,Me}ArNH)$_3$*mes*)Np].OH$_2$. These species are labeled as U-O, Np-O and Np-NH respectively. The results based on electronic energies are shown on the ***left*** while those including enthalpic, solvent and spin-orbit corrections are shown on the ***right***.

reaction that occurs at room temperature. It is possible that the differences between our results and those of Meyer et al. are due to the use of different DFT functionals. We used the PBE-D3BJ functional and have recently shown that PBE provides good agreement with high-accuracy wave-function theory methods for the structures, redox reactivities and energetics of actinide species.[35] With our protocol, the rate-determining barrier is 18.7 kcal/mol, indicating that the overall reaction is feasible at room temperature for [((^{Ad,Me}ArO)$_3$*mes*)U].OH$_2$.

To examine the impact of Np-O → Np-N ligand modulation on the profile of the HER reaction, the actinide-oxo groups in [((^{Ad,Me}ArO)$_3$*mes*)Np].OH$_2$ are converted to actinide-imido groups in [((^{Ad,Me}ArNH)$_3$*mes*)Np].OH$_2$ rather than actinide-amide interactions to avoid steric clashes. From an electronic structure perspective, we find that the Mayer bond order of the activated O-H bond in [((^{Ad,Me}ArNH)$_3$*mes*)Np].OH$_2$ is 1.3% smaller than the bond order of the similar bond in [((^{Ad,Me}ArO)$_3$*mes*)Np].OH$_2$.[50] The decrease in the covalency is confirmed by topological

analysis with the quantum theory of atoms in molecules, see Supporting Information.[51,52] We can thus conclude that the activated O-H bond is slightly stronger in the Np-O complex than in the Np-NH complex. Interestingly, the RDS barrier is 2.6 kcal/mol lower for the Np-NH complex than for [((^{Ad,Me}ArO)$_3$*mes*)Np].OH$_2$, Figure 2. The RDS barrier for the Np-NH complex is 26.7 kcal/mol, to be compared with 29.3 kcal/mol for the Np-O species and 18.7 kcal/mol for the U-O complex. Based on these results, the HER would be significantly faster for U than for the Np species. We also conclude that Np-O → Np-N ligand modulation provides a marginal improvement in the RDS barrier.

We see a similar degree of improvement for the barrier of the second proton abstraction step, Figure 2. For [((^{Ad,Me}ArO)$_3$*mes*)Np].OH$_2$, the TS2 barrier is 6.8 kcal relative to the intermediate complex, while for [((^{Ad,Me}ArNH)$_3$*mes*)Np].OH$_2$, this barrier is only 2.5 kcal/mol. This is an improvement of 4.3 kcal/mol. The magnitude of this improvement remains largely unchanged when we considered only electronic energies, 3.8 kcal/mol, Figure 2. The TS2 barriers for these Np species are to be compared to 4.8 kcal/mol for [((^{Ad,Me}ArO)$_3$*mes*)U].OH$_2$.

The energies for the first proton abstraction step and the overall reaction are however strongly improved with ligand modulation. The first proton abstraction is exothermic for [((^{Ad,Me}ArO)$_3$ *mes*)U].OH$_2$, -7.5 kcal/mol, but endothermic for [((^{Ad,Me}ArO)$_3$*mes*)Np].OH$_2$, 14.0 kcal/mol, and [((^{Ad,Me}ArNH)$_3$*mes*)Np].OH$_2$, 5.5 kcal/mol. This shows that Np-O → Np-N ligand modulation improves the reaction energy by 8.5 kcal/mol. In a similar manner, the overall reaction energy is improved from +0.4 kcal/mol (endothermic) to -9.0 kcal/mol (exothermic) after Np-O → Np-N ligand substitution. This is again an improvement of about 8.5 kcal/mol. We emphasize that the improvement in the reaction energies after Np-O → Np-N substitution is even larger, 16.7 kcal/mol, when we considered only electronic energies. We therefore conclude that Np-O → Np-N substitution is a valuable approach for improving the reaction energies for the HER by Np species. The overall reaction energies for these Np species are to be compared to -18.2 kcal/mol for [((^{Ad,Me} ArO)$_3$*mes*)U].OH$_2$.

3.1.1. Confirmation of trends for the HER: The calculated trends for [((^{Ad,Me}ArO)$_3$*mes*)U]. OH$_2$, [((^{Ad,Me}ArO)$_3$*mes*)Np].OH$_2$ and [((^{Ad,Me}ArNH)$_3$*mes*)Np].OH$_2$ are confirmed in two ways. First, we performed single-point scalar-relativistic DFT calculations with the hybrid B3LYP-D3BJ functional. With this functional, the reaction barriers are larger and the overall HER is less exothermic. Indeed, for [((^{Ad,Me}ArO)$_3$*mes*)U].OH$_2$, the RDS barrier is 37.2 kcal/mol, Figure

3. This is quite high for a reaction that proceeds under ambient conditions. Most importantly however, B3LYP-D3BJ reproduces the improvement in the RDS barrier and overall reaction energies after Np-O → Np-N substitution. Second, the tris-aryloxide ligands are truncated to methyl groups. For the small tris-methyl complexes, we find that the first hydrogen atom abstraction reaction is still the RDS. Also, the barriers and reaction energies are much favorable for the U complex than for the Np species. Most importantly, Np-O → Np-N ligand substitution improves the RDS barrier by 1.3 kcal/mol. Also, the overall reaction energy is also improved

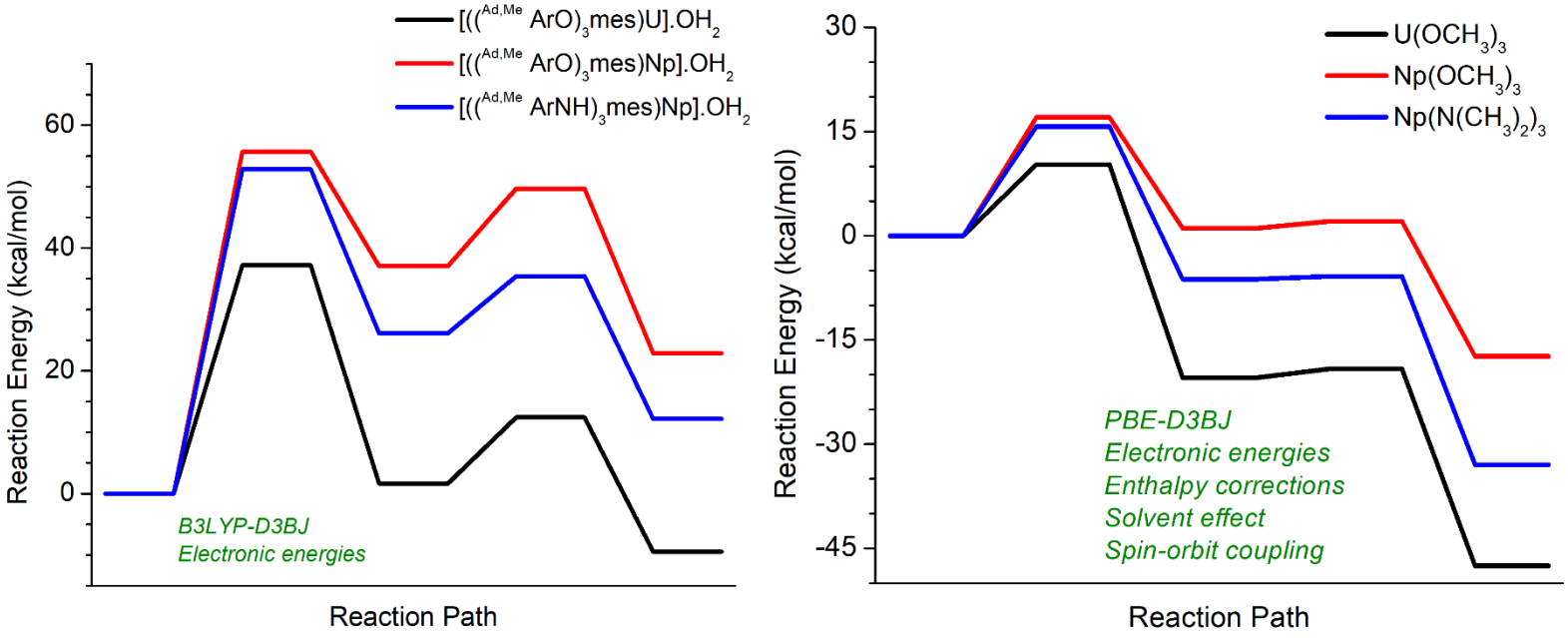

by 15.6 kcal/mol, Figure 3. These results give us confidence regarding the accuracy of the results presented in Figure 2.

Figure 3: (***left***) Reaction profiles for [((^{Ad,Me}ArO)$_3$*mes*)U].OH$_2$, [((^{Ad,Me}ArO)$_3$*mes*)Np].OH$_2$ and [((^{Ad,Me}ArNH)$_3$*mes*)Np].OH$_2$ obtained with the B3LYP-D3BJ functional. (***right***) Reaction profiles obtained for H_2 evolution from water by [U(OMe)$_3$)], [Np(OMe)$_3$)] and [Np(NMe$_2$)$_3$)] obtained with the PBE-D3BJ functional.

3.2. Hydrogen Capture and Hydride Transfer by Bis-Uranium Nitrides: As noted earlier Palumbo et al. recently compared small-molecule activation by bis-uranium nitride complexes, Figure 1.[16] They compared [NBu$_4$][(O)U-N-U(O)] with a OSi(O-*t*-Bu)$_3$) ligand framework, where *t*-Bu = *tert*-butyl, and [NBu$_4$][(N)U-N-U(N)] with a N(SiMe$_3$)$_2$) ligand framework. Specifically, they examined the reactivities of these species with H_2, CO and CO_2. They found that the silylamide, [NBu$_4$][(N)U-N-U(N)], was unreactive towards H_2 while [NBu$_4$][(O)U-N-

U(O)], the siloxide, was able to effect H_2 capture and hydride transfer to yield [NBu_4][(O)U-NH(H)-U(O)]. It thus appears that the empirical observations contradict our computational results that have indicated that An-O → An-N substitutions and ligand modifications leads to improved reactivities for HER and N_2 activation.[17] As such, we have studied [(N)U-N-U(N)][N($SiMe_3$)$_2$)]$^-$ and [(O)U-N-U(O)][OSi(O-*t*-Bu)$_3$)]$^-$. These are the anionic moieties in the silylamide and siloxide complexes, respectively. We consider the structural properties of these moieties as well as their reactivities towards H_2.

3.2.1. Structural and electronic properties: The calculated structural properties of the high-spin quintet (S=2) and open-shell singlet, OSS, (S=0) states of [(O)U-N-U(O)][OSi(O-*t*-Bu)$_3$)]$^-$ and [(N)U-N-U(N)][N($SiMe_3$)$_2$)]$^-$ are compared to parameters from crystal structures in Table 1. The bond distances in the OSS states are longer than those of the quintet states by 0.006-0.023 Å. In contrast, the structural parameters of the quintet states are closer to the parameters from the crystal structures. For the high-spin states, the bond lengths are on average within 0.020 Å of the experiment whereas the bond angles are within 1-4°. This level of agreement gives us good confidence in our computational protocol. The importance of the structural parameters is illustrated by comparing the calculated U-N-U bond angles of [(O)U-N-U(O)][OSi(O-*t*-Bu)$_3$)]$^-$ to experimental data. For the OSS state, the U-N-U angle is almost linear, 179.2°, whereas for the quintet state, we obtained 168.3°, in decent agreement with the experiment.

Table 1: Comparison of the calculated structural properties of [(O)U-N-U(O)][OSi(O-*t*-Bu)$_3$)]$^-$ and [(N)U-N-U(N)][N($SiMe_3$)$_2$)]$^-$ to the crystal structure parameters. Bond lengths are given in Å while bond angles are given in °.

	[(N)U-N-U(N)][N($SiMe_3$)$_2$)]$^-$			[(O)U-N-U(O)][OSi(O-*t*-Bu)$_3$)]$^-$		
	OSS	Quintet	Experiment[16]	OSS	Quintet	Experiment[16]
U-$N_{nitride}$	2.106, 2.107	2.099, 2.090	2.076, 2.083	2.062, 2.071	2.058, 2.073	2.032, 2,067
U-N_{amide}	2.373	2.363	2.35			
U-$O_{siloxide}$				2.176	2.179	2.200
U-U	4.212	4.189	4.159	4.133	4.110	4.090
U-N-U	177.5	177.8	179.0	179.2	168.3	172.2

At the level of theory used in this work, we find that the OSS and quintet states of [(O)U-N-U(O)][OSi(O-*t*-Bu)$_3$)]$^-$ and [(N)U-N-U(N)][N($SiMe_3$)$_2$)]$^-$ are isoenergetic, 0.1-0.8 kcal/mol.

This conforms with the results of Palumbo et al. who used the M06-L and B3LYP functionals.[16] In all cases, we found that the quintet states are more stable than the OSS.

3.2.2. Reaction energies for H_2 capture and hydride transfer: The reaction energies for H_2 capture and hydride transfer by $[(O)U\text{-}N\text{-}U(O)][OSi(O\text{-}t\text{-}Bu)_3)]^-$ and $[(N)U\text{-}N\text{-}U(N)][N(SiMe_3)_2)]^-$ are presented in Table 2. For $[(N)U\text{-}N\text{-}U(N)][N(SiMe_3)_2)]^-$, the reaction energy and enthalpy are +10.0 and +12.6 kcal/mol, respectively, at the PBE/L1 level. Single-point calculations with all-electron TZ2P basis sets and the ZORA approach yields reaction energies of +6.0 and +8.3 kcal/mol at the scalar-relativistic and spin-orbit coupling levels, respectively. As such, we conclude that this silylamide will not capture H_2 and initiate hydride transfer. In contrast, for $[(O)U\text{-}N\text{-}U(O)][OSi(O\text{-}t\text{-}Bu)_3)]^-$, the reaction energies and enthalpies are negative. This indicates that this siloxide complex would be capable of capturing H_2 and initiating hydride transfer. The difference between the reactivities of the siloxide and the silylamide towards H_2 conforms well with the experimental observations.[16] Our computational protocol is able to distinguish cases where ligand substitution leads to improved reaction energies (activation of H_2O and N_2) and situations ligand substitution leads to diminished reactivities, H_2 capture and hydride transfer by $[(O)U\text{-}N\text{-}U(O)][OSi(O\text{-}t\text{-}Bu)_3)]^-$ and $[(N)U\text{-}N\text{-}U(N)][N(SiMe_3)_2)]^-$.

Table 2: Calculated reaction energies and enthalpies, kcal/mol, for H_2 capture and hydride transfer by $[(O)U\text{-}N\text{-}U(O)][OSi(O\text{-}t\text{-}Bu)_3)]^-$ and $[(N)U\text{-}N\text{-}U(N)][N(SiMe_3)_2)]^-$.

	$[(N)U\text{-}N\text{-}U(N)][N(SiMe_3)_2)]^-$		$[(O)U\text{-}N\text{-}U(O)][OSi(O\text{-}t\text{-}Bu)_3)]^-$	
	ΔE	ΔH	ΔE	ΔH
Scalar-relativistic				
PBE/L1	+10.0	+12.6	-11.0	-7.0
PBE-D3BJ/TZ2P	+6.0		-16.1	
Spin-orbit coupling				
PBE-D3BJ/TZ2P	+8.3		-18.2	

To explain the disparity between the siloxide and silylamide species, we consider a pathway that starts with an adduct of H_2 to the U-N-U core, Figure 4. This is followed by dissociation of H_2, transfer of a proton to the nitrido and an hydride to a U center. The intermediate HU-NH-U species has a near-linear U-N-U angle. This species then undergoes structural re-organization to form the final U-(H)(NH)-U product with a bent U-N-U angle, Figure 4. The adduct between

H_2 and $[(N)U\text{-}N\text{-}U(N)][N(SiMe_3)_2)]^-$ is uphill by 8.1 kcal/mol, due to steric constraints. Formation of the intermediate is uphill by an additional 2.2 kcal/mol. Interestingly, re-organization to final product is downhill by just -0.3 kcal/mol. These results show that the reaction energy of $[(N)U\text{-}N\text{-}U(N)][N(SiMe_3)_2)]^-$ is dominated by the repulsive interactions with H_2 in the adduct. During reorganization of the intermediate, the U-N-U core is not sufficiently flexible to account for the repulsive nature of the first phase, Figure 4. We now examine a similar path for $[(O)U\text{-}N\text{-}U(O)][OSi(O\text{-}t\text{-}Bu)_3)]^-$. Here, formation of the adduct is uphill by only

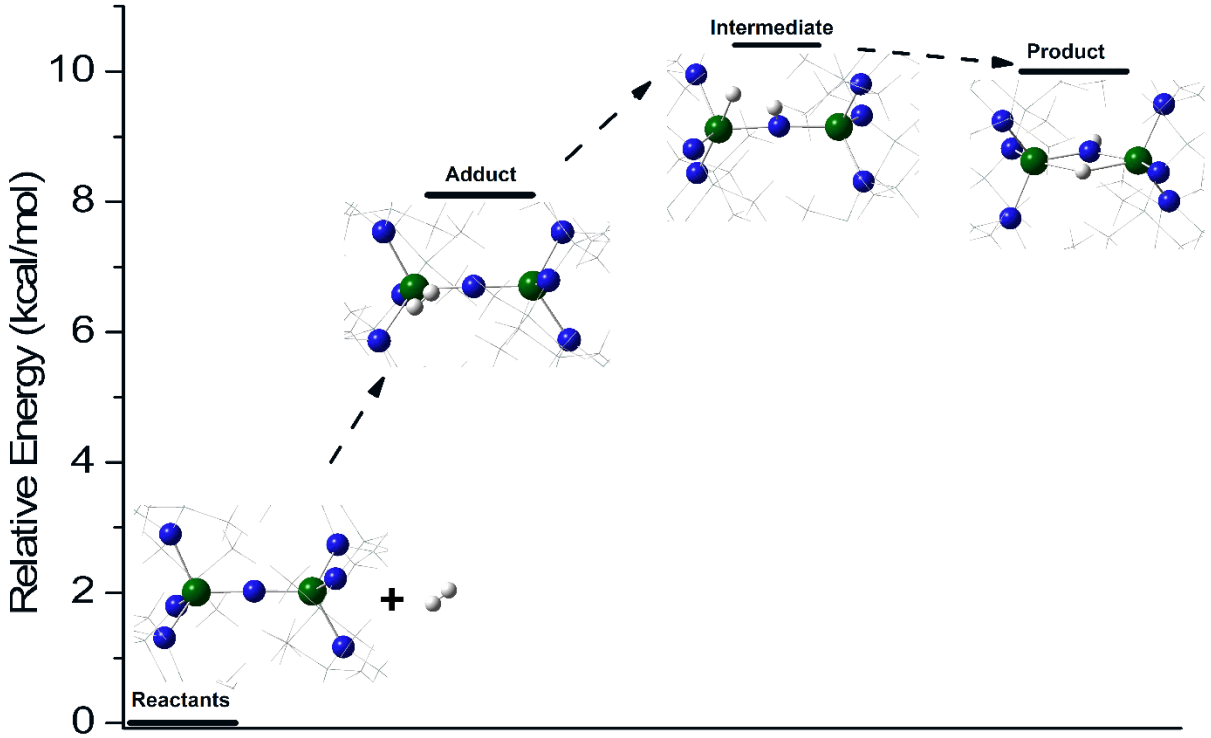

Figure 4: Calculated pathway for H_2 capture and hydride transfer by $[(N)U\text{-}N\text{-}U(N)][N(SiMe_3)_2)]^-$ obtained at the PBE/L1 level of theory.

0.6 kcal/mol, Figure 5. This conforms with the fact that the environment around the bis-uranium nitride core of $[(O)U\text{-}N\text{-}U(O)][OSi(O\text{-}t\text{-}Bu)_3)]^-$ is less confining than that of $[(N)U\text{-}N\text{-}U(N)][N(SiMe_3)_2)]^-$. As started earlier, the $Si(Me)_3$ groups are rather close-in to the U-N-U core of the silylamide, whereas the siloxide has a Si-O spacer between the U-N-U core and t-Bu groups.[16] Formation of the intermediate is uphill by 0.6 kcal for $[(O)U\text{-}N\text{-}U(O)][OSi(O\text{-}t\text{-}Bu)_3)]^-$, compared to 2.2 kcal/mol for the silylamide. However, reorganization of the intermediate is downhill by -11.5 kcal/mol for the siloxide, to be contrasted with only -0.3 kcal/mol for the silylamide. The U-N-U core in the intermediate species of the siloxide is thus sufficiently flexible to drive the whole reaction towards exothermicity.

3.2.3. H_2 capture and hydride transfer by Np analogues: The reaction energies for H_2 capture by $[(O)Np\text{-}N\text{-}Np(O)][OSi(O\text{-}t\text{-}Bu)_3)]^-$ and $[(N)Np\text{-}N\text{-}Np(N)][N(SiMe_3)_2)]^-$ are shown in Table 3. Overall, the reaction energies for the Np species are very similar to those of their U analogues, Table 2. This contrasts greatly with the results obtained for the HER where the barriers and reaction energies were more favorable for U. Crucially, for the HER, the oxidation states of the actinides are changed from +3 to +5. In contrast, for H_2 capture the actinide oxidation states

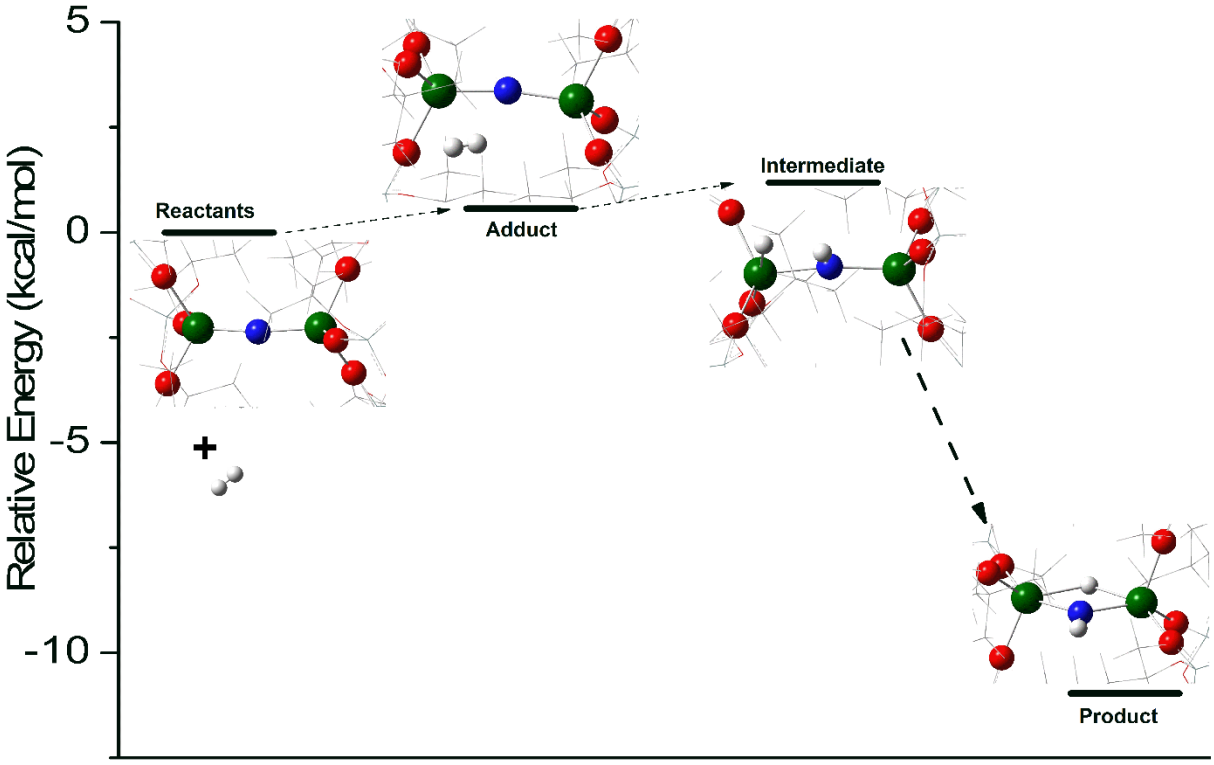

Figure 5: Calculated pathway for H_2 capture and hydride transfer by $[(O)U\text{-}N\text{-}U(O)][OSi(O\text{-}t\text{-}Bu)_3)]^-$ obtained at the PBE/L1 level of theory.

Table 3: Calculated reaction energies and enthalpies, kcal/mol, for H_2 capture and hydride transfer by $[(O)Np\text{-}N\text{-}Np(O)][OSi(O\text{-}t\text{-}Bu)_3)]^-$ and $[(N)Np\text{-}N\text{-}Np(N)][N(SiMe_3)_2)]^-$.

	$[(N)Np\text{-}N\text{-}Np(N)][N(SiMe_3)_2)]^-$		$[(O)Np\text{-}N\text{-}Np(O)][OSi(O\text{-}t\text{-}Bu)_3)]^-$	
	ΔE	ΔH	ΔE	ΔH
Scalar-relativistic				
PBE/L1	+10.5	+14.3	-10.6	-8.7
PBE-D3BJ/TZ2P	+6.2		-13.6	
Spin-orbit coupling				
PBE-D3BJ/TZ2P	+5.2		-15.3	

are unchanged from +4. Thus Np behaves in a similar manner as U for small-molecule activation reactions that do not involve redox transformation of the actinide center.

3.2.4. Like-for-like ligand transformation: The reaction energies for H_2 capture and hydride transfer by $[(N)U\text{-}N\text{-}U(N)][(HN)Si(O\text{-}t\text{-}Bu)_3)]^-$ are compared to those of $[(O)U\text{-}N\text{-}U(O)][OSi(O\text{-}t\text{-}Bu)_3)]^-$ in Figure 6. In $[(N)U\text{-}N\text{-}U(N)][(NH)Si(O\text{-}t\text{-}Bu)_3)]^-$, the U-O bonds of $[(O)U\text{-}N\text{-}U(O)][OSi(O\text{-}t\text{-}Bu)_3)]^-$ are transformed into U-NH groups. Comparison of the reaction energies for these molecules allows a *like-for-like* comparison of the impact of An-O → An-NH actinide-ligand modulation. The steric environments in these two species are largely similar. The results for the Np analogues are also presented.

The calculated reaction energies for $[(N)U\text{-}N\text{-}U(N)][(NH)Si(O\text{-}t\text{-}Bu)_3)]^-$ and its Np analogue are -3.2 and -2.5 kcal/mol, respectively. These are exothermic and are to be compared with $[(N)U\text{-}N\text{-}U(N)][N(SiMe_3)_2)]^-$ and $[(N)Np\text{-}N\text{-}Np(N)][N(SiMe_3)_2)]^-$, for which H_2 capture and hydride transfer is endothermic, Figure 6. This confirms that $[(N)U\text{-}N\text{-}U(N)][N(SiMe_3)_2)]^-$ and $[(N)Np\text{-}N\text{-}Np(N)][N(SiMe_3)_2)]^-$ can not capture H_2 due to the steric confinement of their ligand frameworks. The inability of these species to capture H_2 is not due to the presence of the

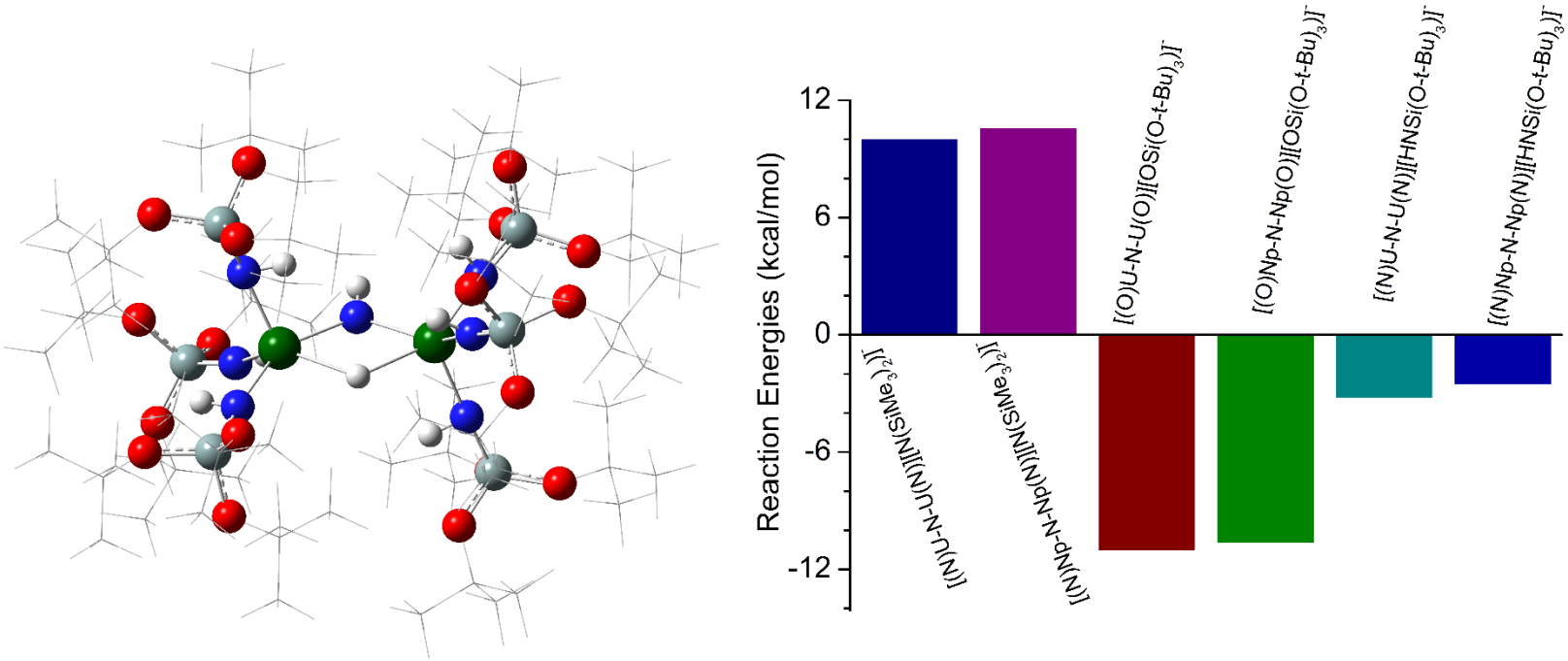

Figure 6: The structure of $[(N)U\text{-}(H)(NH)\text{-}U(N)][(NH)Si(O\text{-}t\text{-}Bu)_3)]^-$ is shown on the ***left***. This species is formed after H_2 capture and hydride transfer by $[(N)U\text{-}N\text{-}U(N)][(NH)Si(O\text{-}t\text{-}Bu)_3)]^-$. The reaction energies for H_2 capture and hydride transfer by various species are shown on the ***right***.

actinide-amide bonds. By comparing [(N)U-N-U(N)][(NH)Si(O-*t*-Bu)$_3$)]$^-$ and [(O)Np-N-Np (O)][OSi(O-*t*-Bu)$_3$)]$^-$, we see that the U-O-Si-O group is more conducive for reorganization than the U-NH-Si-O moiety. As we have previously shown for N_2 activation, we expect that H_2 capture would be even more facile for species containing U-NH-Si-NH groups.[17]

4. CONCLUSIONS

Using scalar-relativistic and spin-orbit coupling DFT calculations, we have investigated small-molecule activation by organometallic uranium (U) and neptunium (Np) complexes. We focus on the impact of An-O → An-N ligand substitution on the reactivities of actinide complexes towards small molecules. An-O depicts actinide-oxo bonds whereas An-N depicts actinide-imido/amide interactions. Specifically we have examined two reactions: *First*, we examined the reaction pathway of the hydrogen evolution reaction (HER) from water. This is motivated by recent work showing that An-O → An-N ligand substitution leads to improved reactivities for neptunium complexes in the four-electron reduction of N_2. Herein, we aim to determine if this trend extends to reactivity with water. *Second*, we compare H_2 capture and hydride transfer by various bis-actinide silylamide and siloxide complexes. Recent experimental work has shown that while the siloxides are reactive towards H_2, the silylamides are not, suggesting that An-O → An-N ligand substitution does not lead to improved reactivities. This seemingly conflicts with our previous results. Thus, we sought to explain the discrepancy and also determine whether our computational protocol could differentiate situations in which ligand substitution leads to improved or diminished reactivities.

For the electrocatalytic reduction of water, HER, we considered U and Np tris-aryloxide complexes. A previous experimental report demonstrated that the U complex, [((^{Ad,Me}ArO)$_3$ *mes*)U].OH$_2$, can effect the HER. This is supported by our calculated reaction energies and barriers. The rate-determining step barrier is on the order of 18.7 kcal/mol for this complex. By contrast, the reaction barriers are significantly higher for [((^{Ad,Me}ArO)$_3$*mes*)Np].OH$_2$. Additionally, the overall reaction is endothermic for the neptunium complex. We find that Np-O → An-NH ligand substitution leads to marginally lower barriers (1-4 kcal/mol) and improved reaction energies (more exothermic by 9-15 kcal/mol). The trends in the barriers and reaction energies seem to be slightly correlated with the Mayer bond order of the activated O-H bonds of water.

For H_2 capture, our computational protocol sufficiently reproduces the experimental structural properties of the bis-uranium nitride, U-N-U, complexes with silylamide, [(N)U-N-U(N)][N(Si $Me_3)_2$)]$^-$, or siloxide, [(O)U-N-U(O)][OSi(O-*t*-$Bu)_3$)]$^-$, ligands. H_2 capture by [(O)U-N-U(O)][O Si(O-*t*-$Bu)_3$)]$^-$ is significantly exothermic while it is strongly endothermic for the [(N)U-N-U(N)][N(Si $Me_3)_2$)]$^-$. Based on these results, we expect that reactivity for H_2 capture and hydride transfer will occur for the former and not for the latter. This conclusion agrees with the experimental observations. We found that the reactivities of the Np analogues are very similar to those of the U complex. This contrasts to the situation observed for water activation. We rationalize this as due to the fact that water activation involves redox transformation of the actinide sites (+3 → +5 oxidation states) while the oxidation states of the actinides remain unchanged during H_2 capture.

We however emphasize that the ligand environments of [(N)U-N-U(N)][N($SiMe_3)_2$)]$^-$ and [(O)U-N-U(O)][OSi(O-*t*-$Bu)_3$)]$^-$ are significantly different. The ligand environment around the U-N-U core of this silylamide is more crowded. This leads to far greater repulsive interactions with H_2 than in the [(O)U-N-U(O)][OSi(O-*t*-$Bu)_3$)]$^-$. Additionally, the final reorganization step is more downhill for the siloxide than for the silylamide. We find that if we simply replaced the U-O bonds in [(O)U-N-U(O)][OSi(O-*t*-$Bu)_3$)]$^-$ with U-NH bonds, reactivity towards H_2 is established. This confirms that [(N)U-N-U(N)][N($SiMe_3)_2$)]$^-$ is un-reactive towards H_2, not because of An-O → An-N ligand substitution, but because the ligand framework is unconducive for this reaction.

For Np complexes, small-molecule activation processes involving redox transformation of the metal site are generally associated with high transition state barriers and endothermicity. Our computations suggest that An-O → An-N ligand substitution provides an opportunity for modest gains in the kinetics as well as substantial gains in the overall reaction energies. There is thus an opportunity for large-scale computational screening of Np complexes that can be useful for catalytic activation of various small molecules. Emphasis should be placed on ligands that can furnish lower activation barriers.

■ ASSOCIATED CONTENT

Supporting Information.

The SI contains the optimized geometries of all the molecules considered in this work. This material is available free of charge via the Internet at http://pubs.acs.org.

AUTHOR INFORMATION

Corresponding Authors

*S.O.O.: E-mail: sodoh@unr.edu

Notes

¶ These authors contributed equally to this work. We declare no competing financial interest.

ACKNOWLEDGMENT

This material is based upon work supported by the National Science Foundation under Grant No. 1800387.

REFERENCES

(1) Arnold, P. L. Uranium-mediated activation of small molecules. *Chem. Commun.* **2011**, *47*, 9005.

(2) Arnold, P. L.; Turner, Z. R. Carbon oxygenate transformations by actinide compounds and catalysts. *Nat. Rev. Chem.* **2017**, *1*, 0002.

(3) Arnold, P. L.; Turner, Z. R.; Germeroth, A. I.; Casely, I. J.; Nichol, G. S.; Bellabarba, R.; Tooze, R. P. Carbon monoxide and carbon dioxide insertion chemistry of f-block N-heterocyclic carbene complexes. *Dalton T.* **2013**, *42*, 1333.

(4) Barluzzi, L.; Falcone, M.; Mazzanti, M. Small molecule activation by multimetallic uranium complexes supported by siloxide ligands. *Chem. Commun.* **2019**, *55*, 13031.

(5) Bart, S. C.; Anthon, C.; Heinemann, F. W.; Bill, E.; Edelstein, N. M.; Meyer, K. Carbon dioxide activation with sterically pressured mid- and high-valent uranium complexes. *J. Am. Chem. Soc.* **2008**, *130*, 12536.

(6) Castro-Rodriguez, I.; Meyer, K. Small molecule activation at uranium coordination complexes: control of reactivity via molecular architecture. *Chem. Commun.* **2006**, 1353.

(7) Falcone, M.; Barluzzi, L.; Andrez, J.; Fadaei Tirani, F.; Zivkovic, I.; Fabrizio, A.; Corminboeuf, C.; Severin, K.; Mazzanti, M. The role of bridging ligands in dinitrogen reduction and functionalization by uranium multimetallic complexes. *Nat. Chem.* **2019**, *11*, 154.

(8) Falcone, M.; Chatelain, L.; Scopelliti, R.; Mazzanti, M. CO cleavage and CO_2 functionalization under mild conditions by a multimetallic CsU_2 nitride complex. *Chimia* **2017**, *71*, 209.

(9) Falcone, M.; Chatelain, L.; Scopelliti, R.; Zivkovic, I.; Mazzanti, M. Nitrogen reduction and functionalization by a multimetallic uranium nitride complex. *Nature* **2017**, *547*, 332.

(10) Falcone, M.; Poon, L. N.; Tirani, F. F.; Mazzanti, M. Reversible dihydrogen activation and hydride transfer by a uranium nitride complex. *Angew. Chem. Int. Edit.* **2018**, *57*, 3697.

(11) Franke, S. M.; Tran, B. L.; Heinemann, F. W.; Hieringer, W.; Mindiola, D. J.; Meyer, K. Uranium(III) Complexes with Bulky Aryloxide Ligands Featuring Metal-Arene Interactions and Their Reactivity Toward Nitrous Oxide. *Inorg. Chem.* **2013**, *52*, 10552.

(12) Halter, D. P.; Heinemann, F. W.; Bachmann, J.; Meyer, K. Uranium-mediated electrocatalytic dihydrogen production from water. *Nature* **2016**, *530*, 317.

(13) Halter, D. P.; Heinemann, F. W.; Maron, L.; Meyer, K. The role of uranium-arene bonding in H_2O reduction catalysis. *Nat. Chem.* **2018**, *10*, 259.

(14) La Pierre, H. S.; Meyer, K. In *"Activation of small molecules by molecular uranium complexes" Progress in Inorganic Chemistry, Vol 58*; Karlin, K. D., Ed. 2014; Vol. 58, p 303.

(15) Lam, O. P.; Meyer, K. Uranium-mediated carbon dioxide activation and functionalization. *Polyhedron* **2012**, *32*, 1.

(16) Palumbo, C. T.; Barluzzi, L.; Scopelliti, R.; Zivkovic, I.; Fabrizio, A.; Corminboeuf, C.; Mazzanti, M. Tuning the structure, reactivity and magnetic communication of nitride-bridged uranium complexes with the ancillary ligands. *Chem. Sci.* **2019**, *10*, 8840.

(17) Panthi, D.; Adeyiga, O.; Dandu, N. K.; Odoh, S. O. Nitrogen reduction by multimetallic trans-uranium actinide complexes: A theoretical comparison of Np and Pu to U. *Inorg. Chem.* **2019**, *58*, 6731.

(18) Schmidt, A. C.; Heinemann, F. W.; Kefalidis, C. E.; Maron, L.; Roesky, P. W.; Meyer, K. Activation of SO_2 and CO_2 by trivalent uranium leading to sulfite/dithionite and carbonate/oxalate complexes. *Chem.-Eur. J.* **2014**, *20*, 13501.

(19) Summerscales, O. T.; Cloke, F. G. N. In *Organometallic and Coordination Chemistry of the Actinides*; AlbrechtSchmitt, T. E., Ed. 2008; Vol. 127, p 87.

(20) Zhang, L.; Zhang, C. C.; Hou, G. H.; Zi, G. F.; Walter, M. D. Small-molecule activation mediated by a uranium bipyridyl metallocene. *Organometallics* **2017**, *36*, 1179.

(21) Arnold, P. L.; Dutkiewicz, M. S.; Walter, O. Organometallic neptunium chemistry. *Chem. Rev.* **2017**, *117*, 11460.

(22) Dutkiewicz, M. S.; Farnaby, J. H.; Apostolidis, C.; Colineau, E.; Walter, O.; Magnani, N.; Gardiner, M. G.; Love, J. B.; Kaltsoyannis, N.; Caciuffo, R.; Arnold, P. L. Organometallic neptunium(III) complexes. *Nat. Chem.* **2016**, *8*, 797.

(23) Arnold, P. L.; Hollis, E.; Nichol, G. S.; Love, J. B.; Griveau, J. C.; Caciuffo, R.; Magnani, N.; Maron, L.; Castro, L.; Yahia, A.; Odoh, S. O.; Schreckenbach, G. Oxo-functionalization and reduction of the uranyl ion through lanthanide-element bond homolysis: Synthetic, structural, and bonding analysis of a series of singly reduced uranyl-rare earth 5f(1)-4f(n) complexes. *J. Am. Chem. Soc* **2013**, *135*, 3841.

(24) Faizova, R.; White, S.; Scopelliti, R.; Mazzanti, M. The effect of iron binding on uranyl(v) stability. *Chem. Sci.* **2018**, *9*, 7520.

(25) Lewis, A. J.; Mullane, K. C.; Nakamaru-Ogiso, E.; Carroll, P. J.; Schelter, E. J. The inverse trans influence in a family of pentavalent uranium complexes. *Inorg. Chem.* **2014**, *53*, 6944.

(26) Lewis, A. J.; Nakamaru-Ogiso, E.; Kikkawa, J. M.; Carroll, P. J.; Schelter, E. J. Pentavalent uranium trans-dihalides and -pseudohalides. *Chem. Commun.* **2012**, *48*, 4977.

(27) Odoh, S. O.; Schreckenbach, G. DFT Study of oxo-functionalized pentavalent dioxouranium complexes: Structure, bonding, ligand exchange, dimerization, and U(V)/U(IV) reduction of OUOH and OUOSiH3 complexes. *Inorg. Chem.* **2013**, *52*, 245.

(28) Laikov, D. N. A new class of atomic basis functions for accurate electronic structure calculations of molecules. *Chem. Phys. Lett.* **2005**, *416*, 116.

(29) Laikov, D. N. Neglect of four- and approximation of one-, two-, and three-center two-electron integrals in a symmetrically orthogonalized basis. *J. Comput. Chem.* **2007**, *28*, 698.

(30) Laikov, D. N.; Ustynyuk, Y. A. PRIRODA-04: a quantum-chemical program suite. New possibilities in the study of molecular systems with the application of parallel computing. *Russ. Chem. B+* **2005**, *54*, 820.

(31) Baerends, E. J.; Ziegler, T.; Atkins, A. J.; Autschbach, J.; Bashford, D.; Baseggio, O.; Bérces, A.; Bickelhaupt, F. M.; Bo, C.; Boerritger, P. M.; Cavallo, L.; Daul, C.; Chong, D. P.; Chulhai, D. V.; Deng, L.; Dickson, R. M.; Dieterich, J. M.; Ellis, D. E.; van Faassen, M.; Ghysels, A.; Giammona, A.; van Gisbergen, S. J. A.; Goez, A.; Götz, A. W.; Gusarov, S.; Harris, F. E.; van den Hoek, P.; Hu, Z.; Jacob, C. R.; Jacobsen, H.*et al.*

(32) te Velde, G.; Bickelhaupt, F. M.; Baerends, E. J.; Guerra, C. F.; Van Gisbergen, S. J. A.; Snijders, J. G.; Ziegler, T. Chemistry with ADF. *J. Comput. Chem.* **2001**, *22*, 931.

(33) Perdew, J. P.; Burke, K.; Ernzerhof, M. Generalized gradient approximation made simple. *Phys. Rev. Lett.* **1996**, *77*, 3865.

(34) Van Lenthe, E.; Baerends, E. J. Optimized slater-type basis sets for the elements 1-118. *J. Comput. Chem.* **2003**, *24*, 1142.

(35) Adeyiga, O.; Suleiman, O.; Dandu, N. K.; Odoh, S. O. Ground-state actinide chemistry with scalar-relativistic multiconfiguration pair-density functional theory. *J. Chem. Phys.* **2019**, *151*, 134102.

(36) Clavaguera-Sarrio, C.; Vallet, V.; Maynau, D.; Marsden, C. J. Can density functional methods be used for open-shell actinide molecules? Comparison with multiconfigurational spin-orbit studies. *J. Chem. Phys.* **2004**, *121*, 5312.

(37) Iche-Tarrat, N.; Marsden, C. J. Examining the performance of DFT methods in uranium chemistry: Does core size matter for a pseudopotential? *J. Phys. Chem. A* **2008**, *112*, 7632.

(38) Odoh, S. O.; Schreckenbach, G. Performance of relativistic effective core potentials in DFT calculations on actinide compounds. *J. Phys. Chem. A* **2010**, *114*, 1957.

(39) Odoh, S. O.; Schreckenbach, G. Theoretical study of the structural properties of plutonium(IV) and (VI) complexes. *J. Phys. Chem. A* **2011**, *115*, 14110.

(40) Schreckenbach, G.; Hay, P. J.; Martin, R. L. Density functional calculations on actinide compounds: Survey of recent progress and application to $UO_2X_4^{2-}$ (X = F, Cl, OH) and AnF_6 (An = U, Np, Pu). *J. Comput. Chem.* **1999**, *20*, 70.

(41) Schreckenbach, G.; Shamov, G. A. Theoretical Actinide Molecular Science. *Accounts Chem. Res.* **2010**, *43*, 19.

(42) Grimme, S.; Antony, J.; Ehrlich, S.; Krieg, H. A consistent and accurate ab initio parametrization of density functional dispersion correction (DFT-D) for the 94 elements H-Pu. *J. Chem. Phys.* **2010**, *132*, 154104.

(43) Grimme, S.; Ehrlich, S.; Goerigk, L. Effect of the damping function in dispersion corrected density functional theory. *J. Comput. Chem.* **2011**, *32*, 1456.

(44) Johnson, E. R.; Becke, A. D. A post-Hartree-Fock model of intermolecular interactions: Inclusion of higher-order corrections. *J. Chem. Phys.* **2006**, *124*, 174104.

(45) Van Lenthe, E.; Snijders, J. G.; Baerends, E. J. The zero-order regular approximation for relativistic effects: The effect of spin-orbit coupling in closed shell molecules. *J. Chem. Phys.* **1996**, *105*, 6505.

(46) Chong, D. P. Augmenting basis set for time-dependent density functional theory calculation of excitation energies: Slater-type orbitals for hydrogen to krypton. *Mol. Phys.* **2005**, *103*, 749.

(47) Chong, D. P.; Van Lenthe, E.; Van Gisbergen, S.; Baerends, E. J. Even-tempered slater-type orbitals revisited: From hydrogen to krypton. *J. Comput. Chem.* **2004**, *25*, 1030.

(48) Marenich, A. V.; Cramer, C. J.; Truhlar, D. G. Generalized Born Solvation Model SM12. *J. Chem. Theory Comput.* **2013**, *9*, 609.

(49) Peeples, C. A.; Schreckenbach, G. Implementation of the SM12 Solvation Model into ADF and comparison with COSMO. *J. Chem. Theory Comput.* **2016**, *12*, 4033.

(50) Mayer, I. Bond order and valence indices: A personal account. *J. Comput. Chem.* **2007**, *28*, 204.

(51) Bader, R. F. W. A quantum theory of molecular structure and its applications. *Chem. Rev.* **1991**, *91*, 893.

(52) Kaltsoyannis, N. Does Covalency Increase or Decrease across the Actinide Series? Implications for Minor Actinide Partitioning. *Inorg. Chem.* **2013**, *52*, 3407.

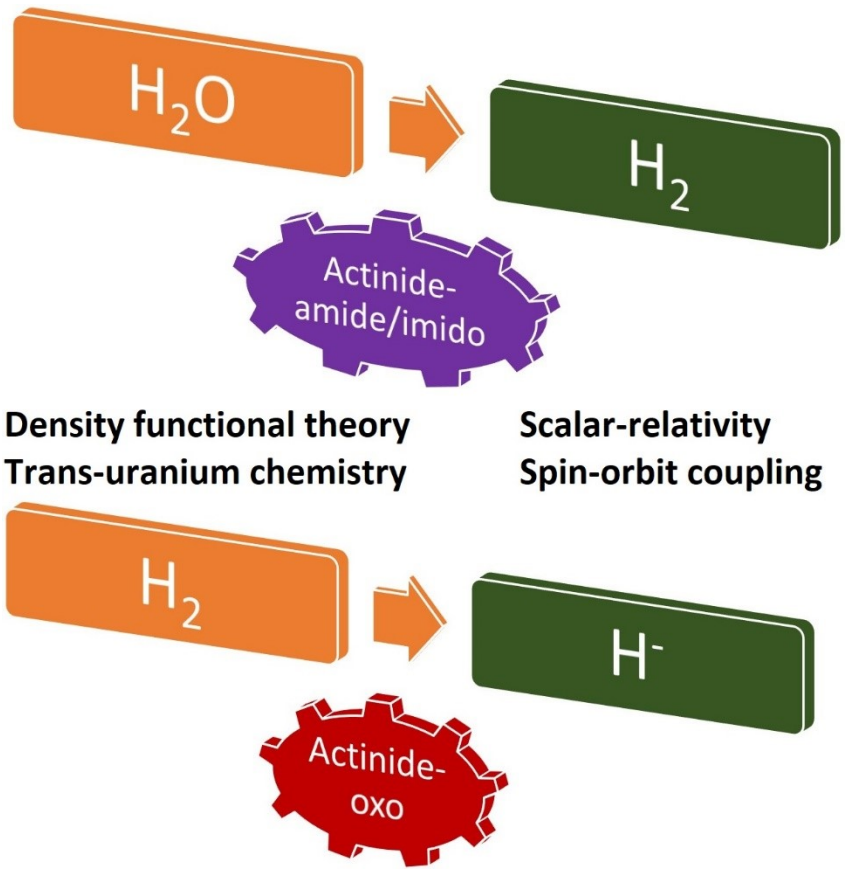

Synopsis: Modification of the ligand environment around the actinide centers provides modest improvement to transition state barriers and significant improvements to overall reaction energy for the hydrogen evolution reaction from water and by neptunium complexes. This conclusion was reached on the basis of spin-orbit coupling density functional theory calculations, suggesting that actinide-oxo → actinide amide/imido substitution is a viable approach for designing trans-uranium complexes useful for small-molecule transformation. We see similar trends for H_2 capture and hydride transfer.